

Experiment no.: HC-2117, **Beamline:** ID 32, **Dates:** 30.08.2016 – 06.09.2016

Local contact: Dr. Flora Yakhou-Harris, **Shifts:** 16

Background and objective

For this experiment we proposed to investigate the magnetisation dynamics within nano-scale magnetic elements by use of holography with extended reference by autocorrelation linear differential operator (HERALDO). The main objective was to obtain time-resolved images of the magnetic vortex cores gyration, induced by use of an RF pulse through a co-planar waveguide (CPW) as well as re-create a previously seen “double Landau” state and obtain images of its dynamics. Overall we were exploring gyrational eigenmodes as well as non-linear effects. In particular we aimed to explore the effect of different geometries on the magnetic dynamics whilst probing the limits of the technique for maximum temporal and spatial resolution achievable at the ID32 beamline.

Results and conclusions

Figures 1, 2a and 2b depict the experimental setup and procedure used within this experiment. Time-resolution was achieved by using the standard stroboscopic pump-probe arrangement where the master clock of the synchrotron facility (probe) was used to trigger the magnetic (pump) RF pulse used to initiate vortex gyration. A delay is introduced between these pump and probe pulses which allows imaging the different phases of the samples internal magnetic state at regular intervals. The facility was running in 16 bunch mode with a probe pulse period of roughly 170 ns, allowing sufficient time for vortex gyration to dampen before the next pump/probe pulse. By using a relatively large RF pulse width of 30 ns allowed us to excite gyration on both the leading and trailing edge of the pulse whilst still leaving enough time between each pulse for sufficient dampening to occur and maintaining the confidence for identifying the exact position of the probe pulse within the pump pulse.

All measurements obtained that utilised the applied bias field were made possible by the integrated electromagnet dipoles present in the chamber on the ID 32 beamline. This setup isn't available to us at any other facility, making ID 32 particularly valuable to us for these measurements. Also, other techniques (e.g. XPEEM) are unable to image with an applied bias field at all as it affects the backscattered electrons that carry the magnetic information within the sample.

The samples used are shown in figure 1, 2c and 2d. It consists of a single column of magnetron sputtered Permalloy (Py) squares (2000 x 2000 x 80 nm) along the central signal line of an integrated gold CPW. The CPW was fabricated using the standard electron beam lithography, thermal evaporation and lift-off process with the following parameters: 4 μm wide central signal line, 75 nm thick and 1 μm separation from the 35 μm ground tracks on either side of the signal line. These were chosen to suit the 50 ohm impedance of the signal generator and SMA cables used. The integrated CPW was connected via gold wire bonds to a standard CPW with an SMA connector. Figure 2d shows the position of the reference slit in the ground strip of the integrated CPW. The slit was milled through the entire sample stack (CPW/membrane/gold mask) via focussed ion beam (FIB) and were 6 μm long and on average 30-40 nm wide. The slit width generally determines the intensity of the interference pattern and the overall resolution of the reconstructed image.

X-ray imaging was performed at 45° to the incident x-ray beam to obtain in-plane magnetic contrast within the sample. Figure 3 shows the field-dependence of the magnetic state within the Permalloy

square. As applied bias field strength is increased the vortex core moves upwards, eventually splitting into two vortices joined by a domain wall. Applied field direction was parallel to the x-ray beam, giving it an x (in-plane) and z (out-of-plane) component for our sample at 45°. The field was then increased to relatively very large values (~4.5 kG) to saturate the samples magnetic state before it was then slowly decreased to zero. As the field strength was decreased a 7-domain state with 2 vortices was consistently formed. This was repeated 3 times and each time ended with the same result. If the starting Landau state was of opposite chirality, the vortex core would move in the opposite direction but formed the same chirality 7-domain state each time. Imaging was done by setting the *Kepeco BOP 100-10MG* power supply to a specific current, collecting images of the static state of the sample then repeating at different Kepeco currents, first increasing sequentially to saturation then decreasing sequentially. Figure 4 shows a comparison between the simulated 7-domain state and the state seen in the experiment. The domain sizes, domain wall shapes and vortex positions correlate well between the two images. Any differences can be attributed to a small remanence bias field.

The next data set was aimed at imaging dynamics of the Landau state with an applied bias field of ~260 G. Figure 5a shows a series of images of the magnetic state within the sample at different delay points. Figure 5b is a plot of the vertical position of the vortex core against the delay time introduced between the x-ray probe and RF pump pulses. We can clearly see the position where the x-ray and RF pulse begin to be synchronised (0 ns delay, was 167 ns on the RF generator). Maximum vertical displacement of the vortex core was about 142 nm (5.4 pixels) after a 3.5 ns delay between the RF and x-ray pulses.

These measurements were repeated with a lower bias field of ~90 G as well as a higher bias field of ~300 G. Figure 6 displays all measurements and a clear gyration is seen in each instance. A gyration period of ~4.5 ns is seen for bias fields of 90 G and 260 G, however a shorter period is seen for the higher bias field of 300 G. This could be because as the core is stretched with the higher field, its tendency to return to its rest position is higher, resulting in a shorter period of gyration. In previous experiments using Py samples of the same size the period of gyration was 4.5 ns so there is good agreement between the results here.

Justification and comments

This is the first time the HERALDO technique has been used to gain high quality images of the field-dependence of nano-scale magnetic elements as well as obtaining time-resolved dynamics whilst using an in-situ bias field. The ID 32 beamline seems to allow us to get information on the samples domain structure as well as the domain walls and have this information separated in the real and imaginary components of the data. This has allowed us to see interesting domain wall structures like the aforementioned domain wall “bubbles” seen in figure 3 with a 90 G bias field. We have also gained knowledge on the functionality of the beamline allowing us to optimise the various coherence-altering slits and undulator gaps to remove specific unwanted artifacts from the collected data and improve contrast of which the origin of such artifacts was previously not particularly clear.

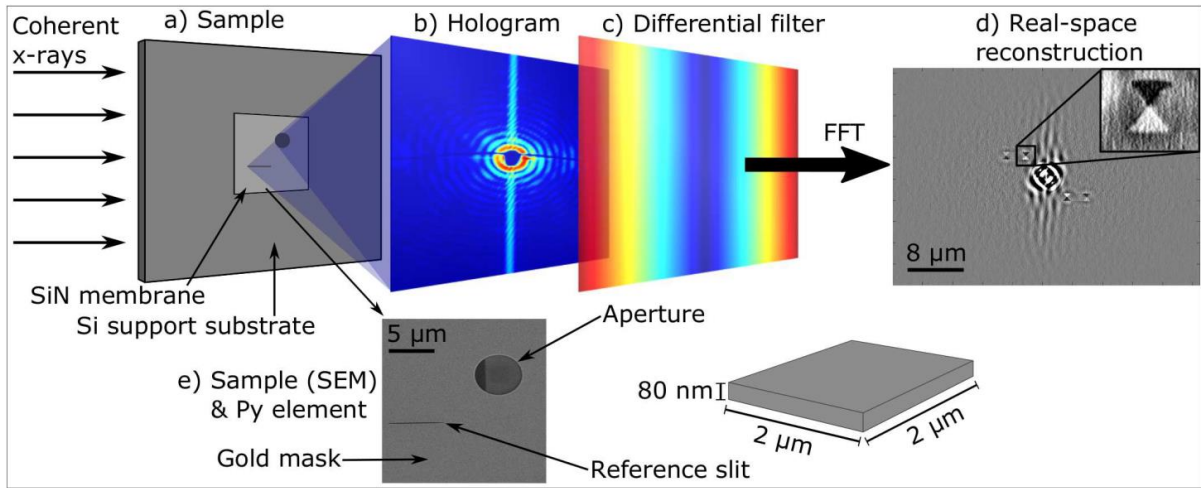


Figure 1: Schematics of the HERALDO setup and sample structure. (a) The SiN membrane containing the sample. The incident x-rays diffract at the aperture hole and the reference slit. (b) The interference between these two beams gives a hologram which is recorded on a CCD camera. (c) The intensity map of the differential filter, applied along the directional derivative of the x-rays from the reference slit. (d) The reconstructed image after fast Fourier transform (FFT) and polarisation analysis. Inset shows a close-up of the aperture with the magnetic contrast of the Py element. (e) Scanning electron microscope (SEM) image from the back side of the sample showing the aperture in the 600 nm gold layer together with the reference slit. The CPW with the square Py element can be seen in the aperture through the 200 nm SiN membrane on the front of the sample.

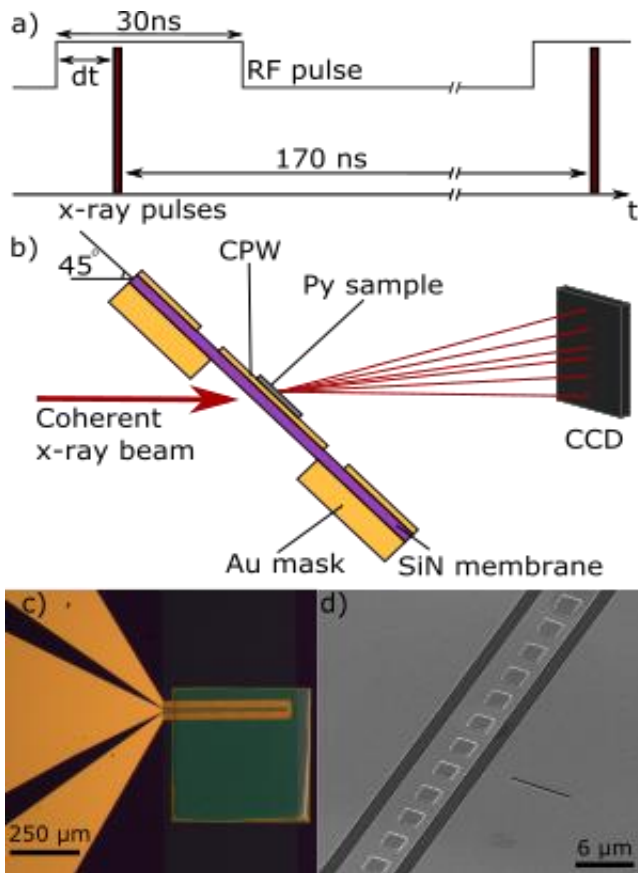


Figure 2: Experimental set-up and time structure of the experiments. (a) Pump-probe time structure used for the stroboscopic imaging. (b) Sample geometry with respect to the x-ray beam for 45° imaging (for perpendicular imaging the sample surface is at 90° to the x-ray beam). (c) Optical image of the sample showing the gold CPW atop the Si substrate and (d) SEM image of the sample showing the gold CPW at the Si substrate.

SiN window. (d) SEM image showing the Py squares, CPW structure and reference slit. The aperture is on the rear side of the sample along the CPW core. Each CPW contains multiple apertures and references separated by $100\ \mu\text{m}$ from each other.

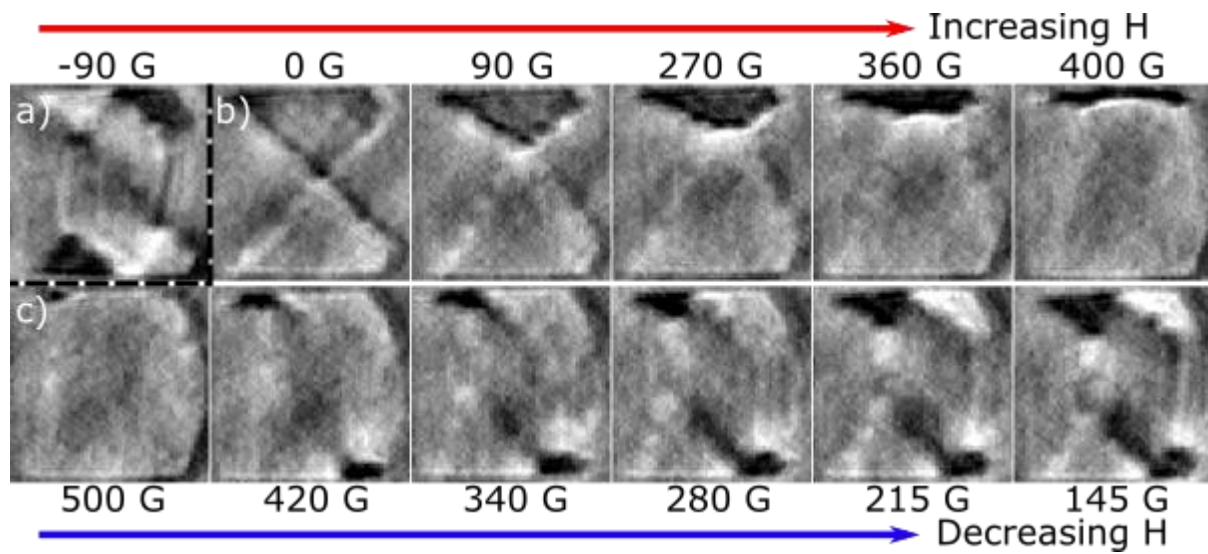


Figure 3: Field-dependence of magnetism within the sample. a) Shows the initial state formed when saturating the sample with a negative bias field and slowly stepping up to zero. b) Once the bias field reaches zero the Landau state reforms, the core then moves upwards with increasing field strength and eventually stretches until it exits the sample and is fully saturated in one direction. c) Upon reducing the applied field strength a 2-vortex (a.k.a 7-domain) state is slowly formed. This state is reproducible as we repeated this hysteresis multiple times and every time this state was reformed.

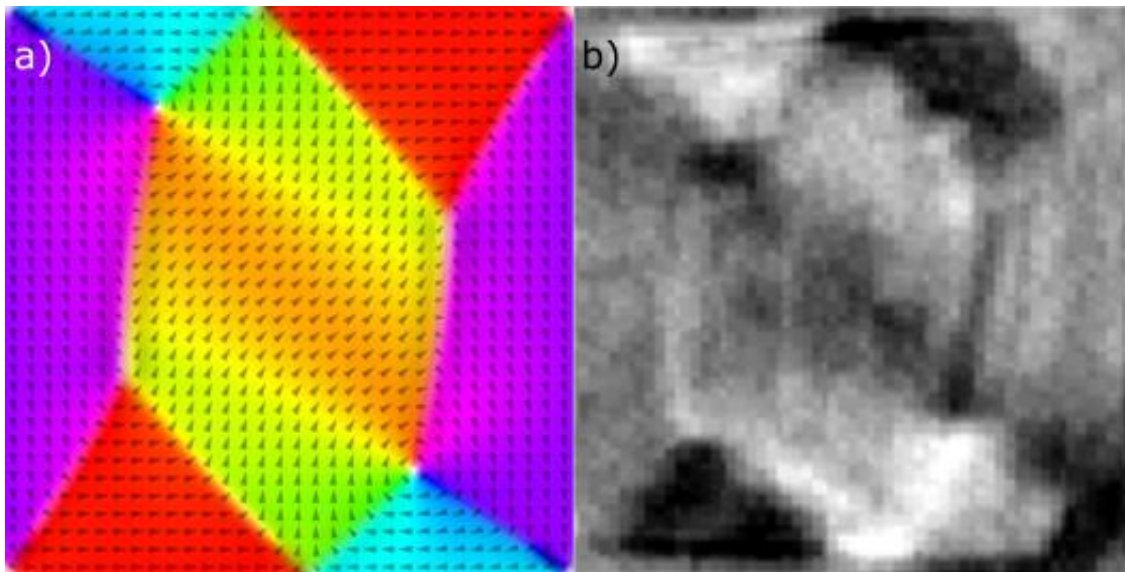


Figure 4: a) simulated and b) experimentally observed 7-domain state. Unfortunately due to the position of the aperture on the sample, the right corners of the Py square are cut off by the gold mask, however the majority of the sample is visible and a clear correlation can be seen between the two images. The vertical domain walls appear to be curved slightly in both instances which is interesting. In the simulation, colour represents xy magnetisation and black-white represents the z-component of magnetism (white points out of the screen, black points into the screen).

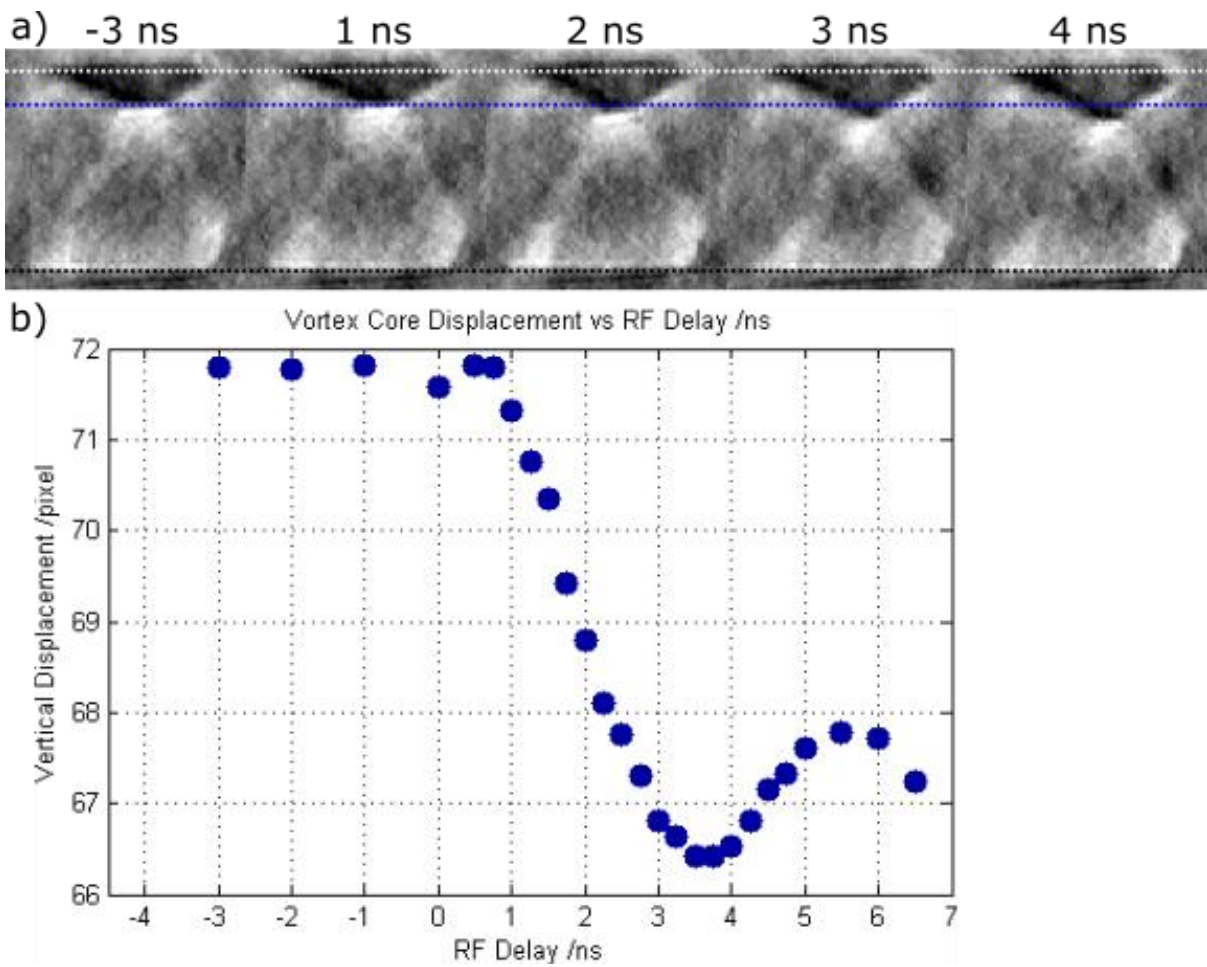


Figure 5: Images of the internal magnetic state of the sample with a 260 G applied bias field at different RF delay times a). A plot of vertical core position against delay time, blue dotted line added to aid in seeing vertical core displacement b) shows a clear oscillation of the vortex core induced by the RF pulse through the CPW. The 250 ps temporal resolution is very clear, we should be able to achieve better temporal resolutions in the future. Vertical displacement on the y-axis is in pixels of which 1 pixel represents ~ 26 nm. Maximum displacement is therefore ~ 142 nm (5.4 pixels) at a delay of 3.5 ns.

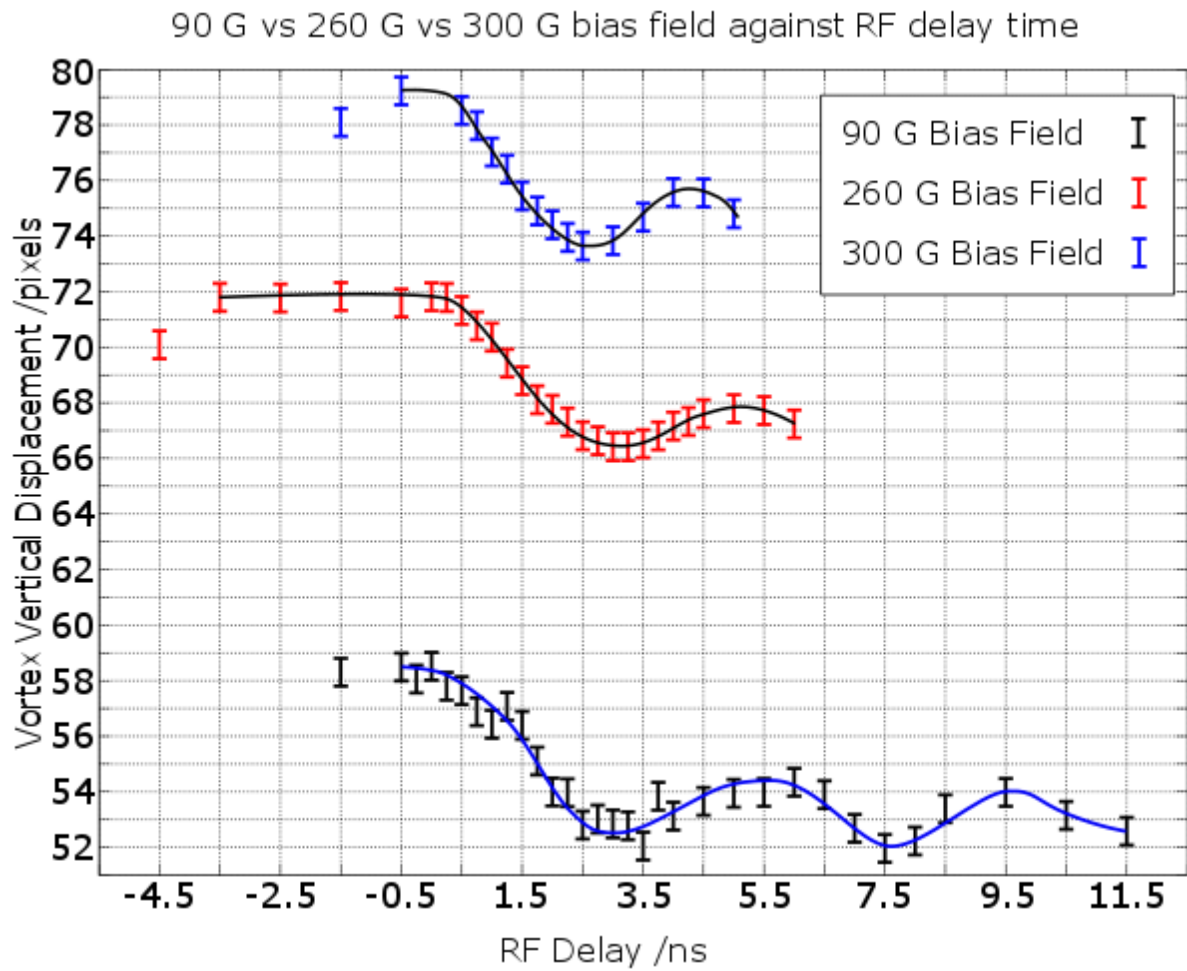


Figure 6: Plot of each of the different bias field strengths and the vertical displacement of the vortex core against RF delay time. Zero RF delay represents the point where the x-ray and RF pulses are synchronised. The 90 G and 260 G bias field strength plots correlate very well with a ~ 4.5 ns peak-to-peak vortex gyration time. The 300 G field however seems to have an increased frequency of gyration at only ~ 3.5 ns. One pixel in the vertical direction represents ~ 27 nm in the sample. Max displacements are ~ 176 nm, 147 nm and 153 nm for 90 G, 260 G and 300 G respectively.